Article

Two-Dimensional Six-Body van der Waals Interactions

Jianing Han

Department of Physics, University of South Alabama, Mobile, AL 36688, USA; jhan@southalabama.edu

Abstract: Van der Waals interactions, primarily attractive van der Waals interactions, have been studied over one and half centuries. However, repulsive van der Waals interactions are less widely studied than attractive van der Waals interactions. In this article, we focus on repulsive van der Waals interactions. Van der Waals interactions are dipole–dipole interactions. In this article, we study the van der Waals interactions between multiple dipoles. Specifically, we focus on two-dimensional six-body van der Waals interactions. This study has many potential applications. For example, the result may be applied to physics, chemistry, chemical engineering, and other fields of sciences and engineering, such as breaking molecules.

Keywords: van der Waals interactions; few-body interactions; dipole–dipole interactions

PACS: 33.20.Bx; 36.40.Mr; 32.70.Jz

1. Introduction

Van der Waals interactions are dipole–dipole interactions [1–8]. For example, we consider a molecule made of two atoms. Each atom in this molecule can be treated as a dipole. Explicitly, the ion core and the valence electron of one atom are the two poles of a dipole. Therefore, the interactions between two atoms are dipole–dipole interactions or van der Waals interactions. In other words, if there is more than one atom, van der Waals interactions exist between those atoms, or van der Waals interactions are very common in three phases of matter. However, one question remains: neutral atoms do not have permanent dipoles. In this article, we will focus on induced-dipole induced-dipole interactions. When two atoms approach each other, the charges within the two atoms will interact with each other, producing induced dipoles. The interactions between those induced-dipoles are van der Waals interactions.

In this article, we use Rydberg atoms to study few-body van der Waals interactions. Rydberg atoms are highly excited atoms, $n > 10$, where n is the principal quantum number. Such atoms have magnified properties, such as greater electric dipole moments compared to ground state atoms, since the radius of an atom is proportional to n^2. In this article, we treat one Rydberg atom [9] as a dipole, the highly excited electron of a Rydberg atom is the negative pole of a dipole, and the ion core of the Rydberg atom is the positive pole of this dipole. Similar to Configuration Interaction (CI) [10], here we consider excited states only.

Repulsive van der Waals interactions have been measured using Atomic Force Microscope (AFM) by intervening liquids between surfaces and between inorganic materials [11,12]; such interactions are combinations of various orders of higher-order interactions. In this article, we consider the near-resonance states, for which the van der Waals interactions are primarily dominant. The repulsive interaction studied in this article is different from the hardcore model described in different textbooks, which is an approximate solution to various orders of higher-order interactions. In this article, we choose a near-resonant state, for which the van der Waals interactions are maximized. Laser cooling and trapping made it possible to directly study repulsive van der Waals interactions in ultracold gases [13–19]. Recently, repulsive van der Waals interactions were discovered in ultracold Rydberg gases [20–22], in which two-body van der Waals interactions were studied. In this article, we focus on six-body interactions. Recently, van der Waals interactions have been

proposed to make more stable quantum gates [23,24]. It has been experimentally tested that repulsive interactions can lead to a longer coherence time [25]. A frequency shift has been observed and explained by a four-body model [26]. However, it was concluded that more atoms need to be taken into account. In this article, we consider six-body interactions.

One possible application of this work is that this may be used to calculate the interactions of molecules with hexagonal structures, including macroscopic molecules composed of highly excited atoms. Another application is to study the interactions within graphene, or Carbon mono-layers, which have a variety of applications [27]. More importantly, the mixing between different states can be used to store quantum information. Furthermore, the results presented can be applied to anti-matters, such as anti-hydrogen, and chemical reactions between anti-matters. For example, the strongest interaction at longer distances between two neutral anti-hydrogen atoms is van der Waals interaction.

2. Theory

The interaction potential energy between two atoms, two dipoles or four charges, is the sum of all pair-wise Coulomb potential energies between the four charges as shown in Figure 1,

$$V_{12} = \frac{e^2}{4\pi\epsilon_0}\left(-\frac{1}{r_1} - \frac{1}{r_2} + \frac{1}{R} + \frac{1}{R'} - \frac{1}{R''} - \frac{1}{R'''}\right). \tag{1}$$
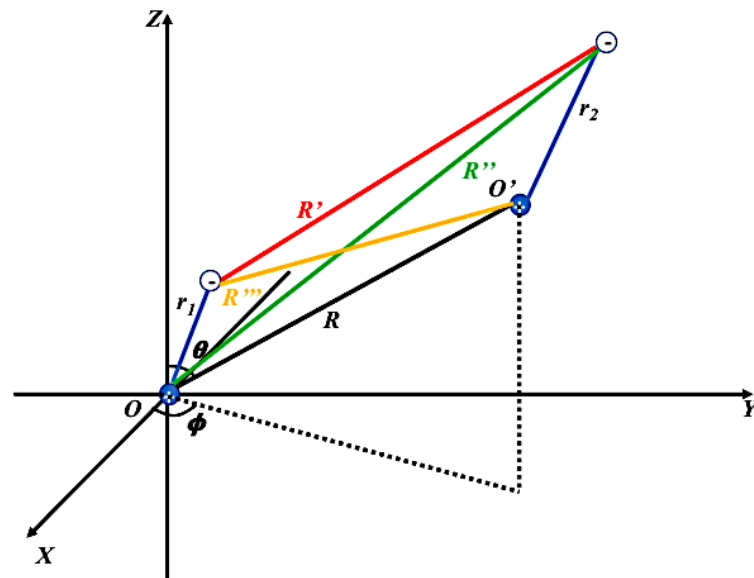
Figure 1. Two ion cores are located at O and O'. The electron of the bottom atom is r_1 (the bottom blue line) away from the bottom ion core, and the electron of the top atom is r_2 (the top blue line) away from the top ion core. R is the distance between the two ion cores. R' (—) is the distance between the two electrons. R'' (—) is the distance between the bottom ion core and the electron of the top atom. R''' (—) is the distance between the electron of the bottom atom and the ion core of the top atom.

In Figure 1, the bottom atom is a dipole, which has one excited electron with charge $-e$ and one ion core with a positive charge e located at the origin of the bottom xyz coordinate. Similarly, the top atom is another dipole. The two poles are the excited electron with charge $-e$ and the ion core with an opposite charge e located at the origin of the top $x'y'z'$ coordinate. $-\frac{e^2}{4\pi\epsilon_0}\frac{1}{r_1}$ is the internal electric potential energy of the bottom atom. Similarly, $-\frac{e^2}{4\pi\epsilon_0}\frac{1}{r_2}$ is the internal potential energy of the top atom. The rest of the equation, $\frac{e^2}{4\pi\epsilon_0}\left(\frac{1}{R} + \frac{1}{R'} - \frac{1}{R''} - \frac{1}{R'''}\right)$, is the potential energy between the two atoms, or two dipoles. If we do Taylor expansion and keep the $\frac{1}{R^3}$ terms, the three-dimensional two-body dipole–

dipole interactions between the top atom, atom 1, and the bottom atom, atom 2, can be written as

$$
\begin{aligned}
V_{12} = \frac{p_1 p_2}{4\pi\epsilon_0 R^3} \{ &-C^1_{1,1}C^2_{1,-1} - C^1_{1,-1}C^2_{1,1} + C^1_{1,0}C^2_{1,0} \\
&- 3[-\frac{1}{\sqrt{2}}sin(\theta)e^{-i\phi}C^1_{1,1} + \frac{1}{\sqrt{2}}sin(\theta)e^{i\phi}C^1_{1,-1} + cos(\theta)C^1_{1,0}] \\
&[-\frac{1}{\sqrt{2}}sin(\theta)e^{-i\phi}C^2_{1,1} + \frac{1}{\sqrt{2}}sin(\theta)e^{i\phi}C^2_{1,-1} + cos(\theta)C^2_{1,0}] \},
\end{aligned}
\tag{2}
$$

where $p_1 = er_1$ and $p_2 = er_2$ are the dipole moments of the atom 1 (or the bottom atom in Figure 1) and atom 2 (or the top atom in Figure 1). r_1 is the radius of the bottom atom or the distance between the ion core and the electron of the bottom atom. Similarly, r_2 is the radius of the top atom. θ is the angle between R and the Z axis, and ϕ is the angle between the projection of R on the XY plane and the X axis. $C_{k,q}$ is the spherical tensor operator [28], and

$$
C_{k,q} = \sqrt{\frac{4\pi}{2k+1}} Y_{kq}(\theta, \phi),
\tag{3}
$$

where $Y_{kq}(\theta, \phi)$ is a kth order spherical harmonic. The superscript on the spherical tensor operator indicates the atom that this operator acts on. If $\theta = 0$ and $\phi = 0$, Equation (2) converts to the very common one-dimensional equation for dipole–dipole interactions [29].

In this article, we considered pair-wise interactions among six bodies. Specifically, we study the dipole–dipole interactions between six excited ^{85}Rb atoms. We will primarily focus on the hexagon configuration shown in Figure 2a, where the six ^{85}Rb atoms are located at the six vertices of the hexagon. In the end, the excitation probability of this configuration is compared to the octahedron case shown in Figure 2b.
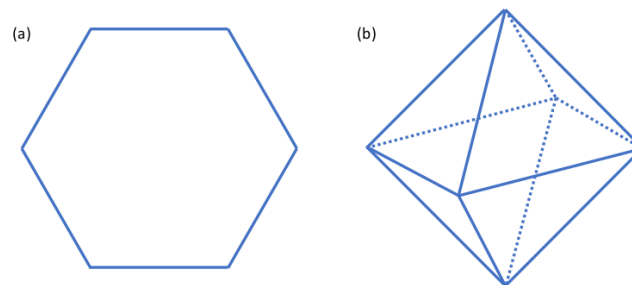
Figure 2. (**a**) A hexagon. The six atoms are located at the six vertices of this hexagon. (**b**) An octahedron. The six atoms are located at the six vertices of this octahedron.

If the six atoms in the hexagon shown in Figure 2a are named atom 1 to 6, respectively. The total potential energy of such a configuration is shown in the following equation [30].

$$
V = \sum_{i<j} V_{ij},
\tag{4}
$$

where i is from 1 to 6, and $i \neq j$. For example, if $i = 1$ and $j = 2$, then V_{ij} is V_{12} as shown in Equation (2), which is the dipole–dipole interaction between atom 1 and atom 2 plotted in Figure 1.

In this calculation, we assume one atom is in $39s$ state, and five atoms are in $38s$ state. For example, the $39s38s38s38s38s38s$ state is strongly coupled with the $38p_{3/2}38p_{3/2}38s38s38s38s$ state through van der Waals interactions [23]. The energy difference between those two states, as the internuclear spacing between two neighboring atoms approaching ∞, is 4.46 MHz, a small difference. Therefore, those states are called near-resonance states. In this calculation, we consider exchange symmetry. For example, all $ssssss$ configurations are considered. Specifically, $39s38s38s38s38s38s$, $38s39s38s38s38s38s$, $38s38s39s38s38s38s$,

$38s38s38s39s38s38s$, $38s38s38s38s39s38s$, and $38s38s38s38s38s39s$ are all taken into account based on the exchange symmetry. In addition, we consider all M states, where M is the projection of the total angular momentum in the Z axis. For example, the M value for the $39s_{1/2,1/2}38s_{1/2,1/2}38s_{1/2,1/2}38s_{1/2,1/2}38s_{1/2,1/2}38s_{1/2,1/2}$ spin-up state is 3. Total 4224 states are included in this calculation. The calculation is done by diagonalizing the Hydrogen-like Hamiltonian matrix elements.

3. Results and Discussion

Figure 3 shows the energy levels calculated for the six-atom configuration shown in Figure 2a by diagonalizing the matrix composed of the possible states described in the theory section. For most levels, it is shown that the energy increases as the internuclear spacing decreases. The corresponding forces, F, are repulsive based on the following equation:

$$\vec{F} = -\nabla V, \tag{5}$$

where V is the potential energy defined in Equation (4), which indicates that the force is state-dependent. ∇ means the divergence of the potential energy. Attractive energy levels are also obtained. However, here we focus on the repulsive energy levels. Unlike the on-resonance dipole–dipole interactions, for which the energy difference between the coupled states is zero as $R \to \infty$, pure repulsive few-body coupled states can be achievable from van der Waals interactions. For example, Figure 4 shows five-body interactions, and the top group of states is purely repulsive [31].
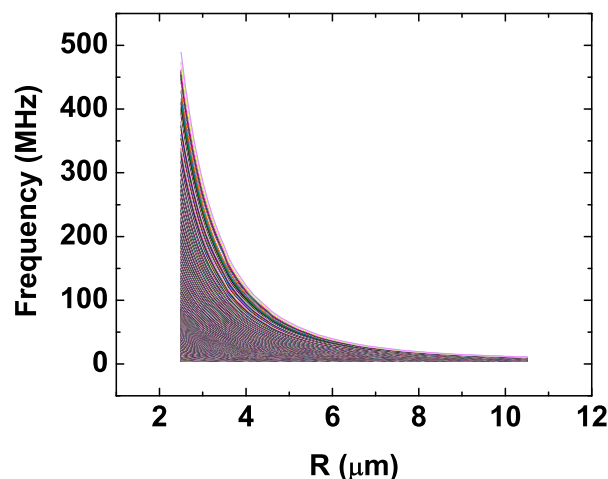

Figure 3. The repulsive energy levels calculated for the hexagon configuration shown in Figure 2a.

The probability of each eigenstate is also investigated. Due to the interactions between the atoms, the atomic eigenstates are no longer the eigenstates of the system. Different states will be mixed, and each state will have a mixing probability. Figure 5 shows the mixing probabilities of different states. Specifically, Figure 5a is the probability for the configuration shown in Figure 2a, and Figure 5b is the probability for the configuration shown in Figure 2b. In this figure, we assume atoms are initially in the *ssssss* states, or the probability of each *ssssss* state is one when R approaches to ∞, where R is the internuclear spacing between neighboring atoms. In addition, it is assumed that the probability in all *ssssss* states is the same. It is shown that the probabilities in different states do not monotonically increase or decrease as the energy increases or decreases. Instead, the probabilities in certain levels are higher than that of the others. This indicates that as the number of atoms increases, the excitation to a single level converts the excitation to energy bands. The higher probabilities indicate that it is possible to excite the atoms to such repulsive states, which leads to repulsive forces between the atoms. Therefore, such states can be used to break molecules. Experimentally, the line shape, which shows broadening and changing shapes caused by few-body interactions, will deviate from the standard

atomic line shape. Such bands are especially useful for superradiance generation. In addition, as a greater number of states are considered, the energy levels are closer to each other, which are closer to energy bands.
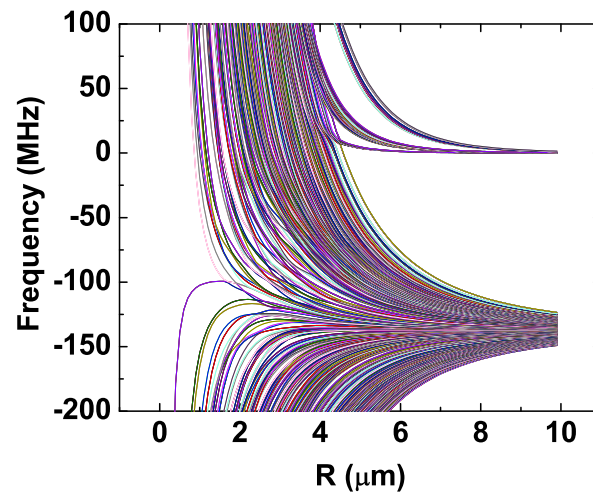
Figure 4. Four atoms are located at the four vertices of a tetrahedron, and one atom is located at the center of the tetrahedron. Two groups of levels are shown. For the top group, there are four $40s$ atoms and one $41s$ atom, and there are three $40s$ atoms and two $40p_{3/2}$ atoms in the bottom group. The horizontal axis is the side length of the tetrahedron. The detailed calculation can be found in Reference [31].
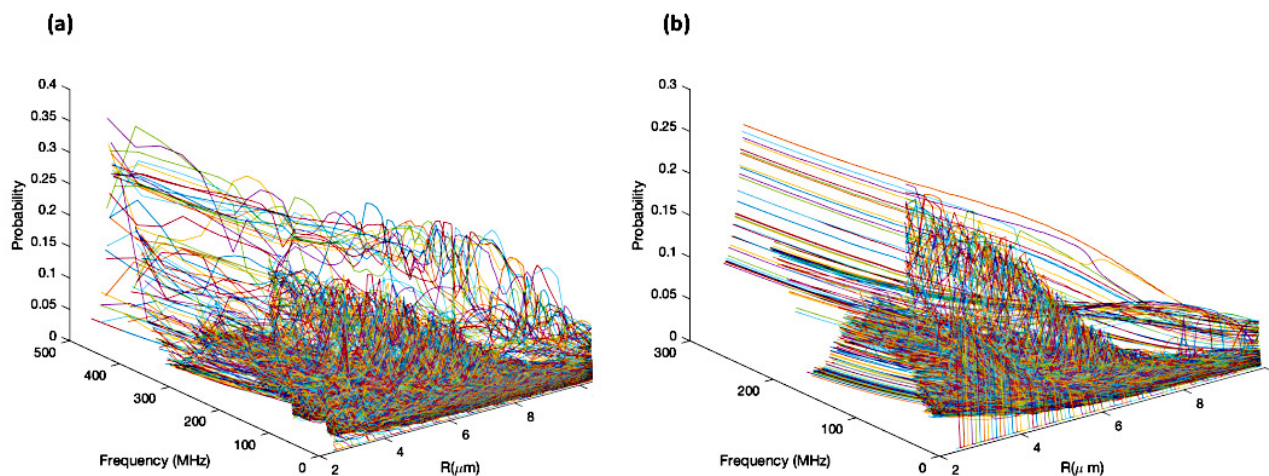
Figure 5. (**a**) The probabilities as a function of the frequency shift and the internuclear spacing R in the states calculated in the hexagon configuration shown in Figure 2a. (**b**) The probabilities as a function of the frequency shift and the internuclear spacing R in the states calculated in the Octahedron configuration shown in Figure 2b.

4. Conclusions

In contrast to previous calculations, this article focuses on two-dimensional six-body interactions among excited atoms, which have not been reported in the past. It has been shown that two-dimensional van der Waals interactions can be repulsive. For example, six-body van der Waals repulsive energy levels have been calculated, and the corresponding probability in each repulsive state is investigated. In addition, it has been shown that a group of energy levels, which are energetically close, has much higher probabilities than other energy levels, which indicates excitation bands can be achievable experimentally. Such calculations show that it is possible to break molecules or to be used to study chemical reactions between anti-matters. In most dissociation processes, ionization is very likely to

happen due to collisions or autoionization. If the atoms are excited to the dipole–dipole coupled purely repulsive states, the dissociation can happen quickly, and ionization can be avoided at certain internuclear spacings.

Institutional Review Board Statement: Not applicable.

Informed Consent Statement: Not applicable.

Data Availability Statement: All data are contained in this article.

Conflicts of Interest: The author declares no conflict of interest.

References

1. Parsegian, V.A. *Van der Waals Forces: A Handbook for Biologists, Chemists, Engineers, and Physicists*; Cambridge University Press: Cambridge, UK, 2006.
2. Smith, E.B.; Tindell, A.R. Faraday Discussions of the Chemical Society: Van der Waals molecules. *R. Soc. Chem.* **1982**, *73*, 19–31.
3. Johnston, D.C. *Advances in Thermodynamics of the van der Waals Fluid*; Morgan & Claypool Publishers: Kentfield, CA, USA, : 2014.
4. London, F. The general theory of molecular forces. *Trans. Faraday Soc.* **1937**, *33*, 8. [CrossRef]
5. Casimir, H.B.G.; Polder, D. Influence of retardation on the London-van der Waals forces. *Phys. Rev.* **1948**, *73*, 360. [CrossRef]
6. Casimir, H.B.G.; Polder, D. Influence of retardation on the London-van der Waals forces. *Nature* **1946**, *158*, 787–788. [CrossRef]
7. Li, W.; Tanner, P.J.; Gallagher, T.F. Dipole-dipole excitation and ionization in an ultracold gas of Rydberg atoms. *Phys. Rev. Lett.* **2005**, *94*, 173001. [CrossRef]
8. Dobson, J.F.; Savin, A.; Angyan, J.G.; Liu, R.F. Spooky correlations and unusual van der Waals forces between gapless and near-gapless molecules. *J. Chem. Phys.* **2016**, *145*, 204107. [CrossRef]
9. Gallagher, T.F. *Rydberg Atoms*; Cambridge University Press: Cambridge, UK, 1994.
10. McGuire, E.J. Completeness in configuration-interaction calculations. *Phys. Rev. A* **1986**, *33*, 1492. [CrossRef]
11. Milling, A.; Mulvaney, P.; Larson, I. Direct Measurement of Repulsive van der Waals Interactions Using an Atomic Force Microscope. *J. Colloid Interface Sci.* **1996**, *180*, 460–465. [CrossRef]
12. Meurk, A.; Luckham, P.F.; Bergström, L. Direct Measurement of Repulsive and Attractive van der Waals Forces between Inorganic Materials. *Langmuir* **1997**, *13*, 3896. [CrossRef]
13. Wineland, D.J.; Drullinger, R.E.; Walls, F.L. Radiation-Pressure cooling of bound resonant absorbers. *Phys. Rev. Lett.* **1978**, *40*, 1639. [CrossRef]
14. Neuhauser, W.; Hohenstatt, M.; Toschek, P.; Dehmelt, H. Optical-Sideband cooling of visible atom cloud confined in parabolic well. *Phys. Rev. Lett.* **1978**, *41*, 233. [CrossRef]
15. Phillips, W.D.; Metcalf, H.J. Cooling and trapping atoms. *Sci. Am.* **1987**, *256*, 50. [CrossRef]
16. Chu, S.; Hollberg, L.; Bjorkholm, J.E.; Cable, A.; Ashkin, A. Three-dimensional viscous confinement and cooling of atoms by resonance radiation pressure. *Phys. Rev. Lett.* **1985**, *55*, 48. [CrossRef] [PubMed]
17. Lett, P.D.; Watts, R.N.; Westbrook, C.I.; Phillips, W.D.; Gould, P.L.; Metcalf, H.J. Observation of Atoms Laser Cooled below the Doppler Limit. *Phys. Rev. Lett.* **1988**, *61*, 169. [CrossRef] [PubMed]
18. Ketterle, W. Nobel lecture: When atoms behave as waves: Bose–Einstein condensation and the atom laser. *Rev. Mod. Phys.* **2002**, *74*, 1131. [CrossRef]
19. Cornell, E.A.; Wieman, C.E. Nobel Lecture: Bose–Einstein condensation in a dilute gas, the first 70 years and some recent experiments. *Rev. Mod. Phys.* **2002**, *74*, 875. [CrossRef]
20. Han, J.; Gallagher, T.F. Millimeter-wave rubidium Rydberg van der Waals spectroscopy. *Phys. Rev. A* **2009**, *79*, 053409. [CrossRef]
21. Teixeira, R.C.; Hermann-Avigliano, C.; Nguyen, T.L.; Cantat-Moltrecht, T.; Raimond, J.M.; Haroche, S.; Gleyzes, S.; Brune, M. Microwave probe dipole blockade and van der Waals forces in a cold Rydberg gas. *Phys. Rev. Lett.* **2015**, *115*, 013001. [CrossRef]
22. Faoro, R.; Simonelli, C.; Archimi, M.; Masella, G.; Valado, M.M.; Arimondo, E.; Mannella, R.; Ciampini, D.; Morsch, O. van der Waals explosion of cold Rydberg clusters. *Phys. Rev. A* **2016**, *93*, 030701(R). [CrossRef]
23. Han, J. Broadband laser excitation of van der Waals polymers from a cold atomic gas. *Mol. Phys.* **2017**, *115*, 2479–2485. [CrossRef]
24. Endres, M. Quantum Science with Alkaline Earth Tweezer Arrays. In *APS Division of Atomic, Molecular and Optical Physics Meeting Abstracts*; College Park, MD, USA, 2020. Available online: https://ui.adsabs.harvard.edu/abs/2020APS..DMPG08003E/abstract (accessed on 20 January 2022).

25. Engels, P. Lattice Experients with Raman dressed Bose–Einstein condensate. In *APS Division of Atomic, Molecular and Optical Physics Meeting Abstracts*; College Park, MD, USA, 2020. Available online: https://ui.adsabs.harvard.edu/abs/2020APS..DMPM08004E/abstract (accessed on 20 January 2022).
26. Han, J. MHz few-body frequency shift detected in a cold 85 Rb Rydberg gas. *Phys. Rev. A* **2011**, *84*, 052516. [CrossRef]
27. Das, S.; Robinson, J.A.; Dubey, M.; Terrones, H.; Terrones, M. Beyond Graphene: Progress in Novel Two-dimensional Materials and van der Waals solids. *Annu. Rev. Mater. Res.* **2015**, *45*, 1–27. [CrossRef]
28. Edmonds, A.R. *Angular Momentum in Quantum Mechanics*; Princeton University Press: Princeton, NJ, USA, 1957.
29. Han, J. Dipole Effects in a Cold Rydberg Gas. Ph.D. Thesis, University of Virginia, Charlottesville, VA, USA, 2009.
30. von Stecher, J.; D'Incao, J.P.; Greene, C.H. Signatures of universal four-body phenomena and their relation to the Efimov effect. *Nat. Phys.* **2009**, *5*, 417–421. [CrossRef]
31. Han, J. Five-body van der Waals interactions. *Phys. Rev. A* **2017**, *95*, 062502. [CrossRef]